A VARIATIONAL APPROACH TO CONTACT ANGLE SATURATION AND CONTACT LINE INSTABILITY IN STATIC ELECTROWETTING

by M. A. FONTELOS[†]

(*Instituto de Ciencias Matemáticas (ICMAT, CSIC-UAM-UCM-UC3M), Consejo Superior de Investigaciones Científicas, C/ Serrano* 123, 28006 *Madrid, Spain*)

and U. KINDELÁN[‡]

(*Departamento de Matemática Aplicada y Met. Inf., Universidad Politécnica de Madrid, Ríos Rosas* 21, 28003 *Madrid, Spain*)

[Received 2 January 2009. Revised 24 May 2009. Accepted 6 June 2009]

Summary

Drops of a conducting fluid in electrowetting devices tend to spread when a difference of potential V_0 is set between the drop and an electrode external to it. The classical Lippmann theory predicts unlimited spreading, with a decrease of the contact angle between drop and solid substrate, as one increases V_0. This fact is in contradiction with current experiments, where saturation of the contact angle to a limiting value is found. A further increase of V_0 does not lead to further spreading but to the appearance of instabilities in the form of emitted drops at the contact line. We provide an explanation to these two related phenomena based solely on interfacial and electrostatic energies. A local analysis close to the contact line is also provided and an expression for the most unstable mode is deduced.

1. Introduction

Electrowetting has become one of the most widely used tools for manipulating tiny amounts of liquids on surfaces. Applications range from 'lab-on-a-chip' devices (**1**) to adjustable lenses and new kinds of electronic displays (**2**, **3**). In the simplest configuration, represented in Fig. 1, a drop of conducting fluid rests over a solid substrate and a difference of potential V_0 is established between the drop and an electrode placed at a distance d for the substrate. This case represents 'static electrowetting' as opposed to 'spontaneous electrowetting' where a spontaneous thin front-running electrowetting film is pulled out ahead of the macroscopic drop with the use of planar parallel line electrodes (cf. (**4**)). Lippmann (**5**) developed a formula, nowadays called Lippmann's law, for the value of the contact angle of the drop under a potential V_0 as a function of Young's angle θ_Y, liquid–gas surface tension coefficient γ_{lv}, the distance between drop and electrode, and the dielectric

[†]Corresponding author. ⟨marco.fontelos@uam.es⟩
[‡]⟨ultano.kindelan@upm.es⟩

Q. Jl Mech. Appl. Math, Vol. 62. No. 4
Advance Access publication 6 July 2009. doi:10.1093/qjmam/hbp016

constant $\varepsilon_0\ \varepsilon_r$ of the medium between electrode and drop:

$$\cos\theta(V_0) = \cos\theta_Y + \frac{\varepsilon_0\varepsilon_r}{2d\gamma_{lv}}V_0^2. \tag{1}$$

Since Lippmann assumed that the drop is a spherical cap, the value of a, the radius of the circular solid–liquid interface, follows immediately from $\theta(V_0)$. Despite the importance of the phenomenon of electrowetting, some of its most important features are not well understood. This is the case of saturation and contact line instability phenomena that are exhibited instead of the unlimited spreading predicted by Lippmann's law when $\cos\theta(V_0) \to 0$. Moreover, once the saturation angle is reached, an increase of V_0 produces instabilities at the contact line that result in the emission of multiple fingers, whose number increases with increasing potential. Various explanations to these phenomena have been proposed, like effects of charge trapping, air ionization or intrinsic material properties of both the drop and the substrate (see, for instance, (**6**)).

In this article, we provide an explanation for the saturation and instability effects, which only needs to invoke interfacial and electrostatic effects. According to our results, these phenomena arise as a consequence of instabilities leading to the breakup of axial symmetry. The manifestation of such instabilities is an undulation of the contact line, sometimes with large wave numbers. We show that the instabilities occur for not very large values of the wetted area and hence represent a limitation of applicability of electrowetting procedures.

The starting point of our analysis is the formula for the energy in the configuration represented in Fig. 1:

$$E = \gamma_{lv}\,[A_{lv} - (\cos\theta_Y)A_{sl}] - \frac{1}{2}CV_0^2, \tag{2}$$

where C represents the electric capacity of the capacitor formed by the drop electrode system; γ_{lv}, the liquid–vapor surface tension and A_{lv} and A_{sl} represent the areas of the liquid–vapor and solid–liquid interfaces, respectively. The equilibrium shape of the drop that occupies a given volume will be such that the energy (2) is minimized. When $V_0 = 0$ the minimizers, of (2) are spherical caps with a contact angle θ_Y. When $V_0 \neq 0$, the minimizers cannot be computed analytically, but for given $\theta_Y \ll 1$, d and $V_0 \ll 1$ the deformation of the drop due to the presence of the electric field should be small, the drop would be very flat so that the capacity of the drop electrode system could be

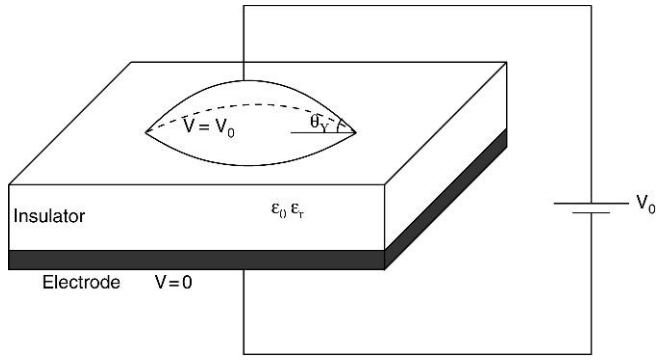

Fig. 1 Sketch of the physical setting

approximated by $C \approx \frac{\varepsilon_0 \varepsilon_r}{2d} A_{sl}$ and the shape would be a spherical cap with contact angle θ following Lippmann's law. Nevertheless, we shall show now that there exist configurations where the circular symmetry of the liquid–solid interface is broken and possessing less energy than the spherical caps predicted by Lippmann's law. For simplicity, we will consider in most of our discussion $\varepsilon_r = 1$. Usually, in experiments, ε_r is chosen larger than 1 and the electric field is increased near the contact line. As we will see, this fact does not change our conclusions.

2. Drops with broken axial symmetry

We introduce cylindrical coordinates, with z being the axis of symmetry of a spherical cap, and an $O(\varepsilon)$ azimuthal perturbation so that

$$r(\theta, z) = \frac{a(z)}{\sqrt{1 + \frac{\varepsilon^2}{2}}}(1 + \varepsilon \cos(n\theta)), \tag{3}$$

where $n = 1, 2, \ldots$ represents the perturbed drop's surface (see Fig. 2) and $0 \leqslant z \leqslant H$, with H being the drop's height. We show below that the perturbed shapes (3) produce, under certain conditions on $a(z)$, the energy functional (2) smaller than the axisymmetric counterpart (that is with $\varepsilon = 0$). Notice that the perturbation introduced in (3) makes the resulting shape only Lipschitz continuous at the apex. This is not a problem since both area and capacity are well defined. Then, the liquid–solid interface area remains unchanged as well as the drop's volume, but the liquid–vapor interface area changes an amount

$$\begin{aligned} A_{lv}(\varepsilon) &= \int_0^H \int_0^{2\pi} \sqrt{r^2 + r_\theta^2 + r^2 r_z^2}\, d\theta dz \\ &= \int_0^H \int_0^{2\pi} r\sqrt{1 + r_z^2} \left(1 + \frac{r^{-2} r_\theta^2}{\sqrt{1 + r_z^2} + \sqrt{1 + r^{-2} r_\theta^2 + r_z^2}} \right) d\theta dz \end{aligned}$$

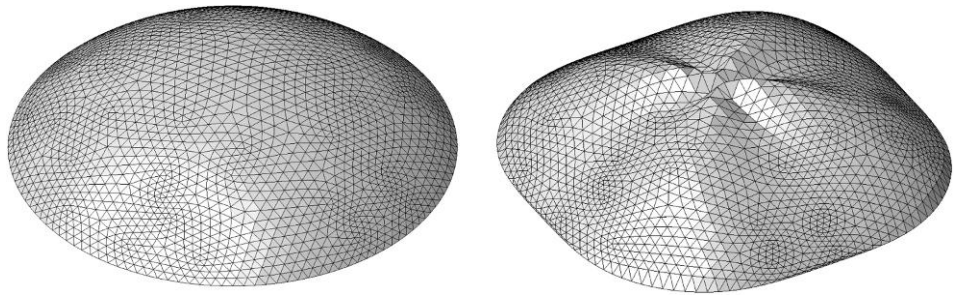

Fig. 2 Triangularization of the drop's surface for axisymmetric shape (left) and the same shape perturbed with a $n = 4$ mode

$$= \int_0^H \int_0^{2\pi} r\sqrt{1+r_z^2}\left(\frac{1+r^{-2}r_\theta^2}{\sqrt{1+r_z^2}+\sqrt{1+r^{-2}r_\theta^2+r_z^2}}\right)d\theta dz$$

$$+ \int_0^H \int_0^{2\pi} r\sqrt{1+r_z^2}\,d\theta dz = I_1 + I_2,$$

where

$$I_1 = \int_0^H \int_0^{2\pi} r\sqrt{1+r_z^2}\left(\frac{1+r^{-2}r_\theta^2}{\sqrt{1+r_z^2}+\sqrt{1+r^{-2}r_\theta^2+r_z^2}}\right)d\theta dz$$

$$\leqslant \int_0^H \int_0^{2\pi} \frac{r}{2}n^2\varepsilon^2\sin^2(n\theta)d\theta dz = n^2\varepsilon^2\frac{\pi}{2}\int_0^H a(z)dz = c_1 n^2\varepsilon^2,$$

and

$$I_2 = \int_0^H \int_0^{2\pi} r\sqrt{1+r_z^2}\,d\theta dz$$

$$= \int_0^H \int_0^{2\pi} a\sqrt{1+a_z^2}\left[1-\frac{\varepsilon^2}{4}+\frac{\varepsilon^2}{2}\frac{a_z^2}{1+a_z^2}-\frac{\varepsilon^2}{4}\frac{a_z^4}{\left(1+a_z^2\right)^2}+O(\varepsilon^3)\right]d\theta dz$$

$$= \int_0^H \int_0^{2\pi} a\sqrt{1+a_z^2}\left[1-\frac{\varepsilon^2}{4}\frac{1}{\left(1+a_z^2\right)^2}+O(\varepsilon^3)\right]d\theta dz$$

$$= A_{lv}(0) + c_2\varepsilon^2 + O(\varepsilon^3).$$

Hence,

$$A_{lv}(\varepsilon) = A_{lv}(0) + \varepsilon^2(c_1 n^2 + c_2) + O(\varepsilon^3), \tag{4}$$

where $c_2 \leqslant 0$ and, for a drop of unit volume,

$$c_1 = \frac{\pi}{2}\int_0^H a\,dz \leqslant \left(\int_0^H \frac{\pi}{4}dz\right)^{\frac{1}{2}}\left(\int_0^H \pi a^2 dz\right)^{\frac{1}{2}} \leqslant \frac{\sqrt{\pi}}{2}H^{\frac{1}{2}}.$$

The capacity of the drop electrode system can be estimated to be

$$C(\varepsilon) = C_0 + \varepsilon^2 C_{n,1} + O(\varepsilon^3), \tag{5}$$

where C_0 is the capacity of the axisymmetric drop and

$$C_{n,1} \geqslant C_{n-1,1} > 0, \tag{6}$$

for all n. The proof of (5) and (6) follows from a calculation similar to Fontelos and Kindelán (**7**), but adapted to take into account the presence of an electrode. We denote Ω as the region occupied by the fluid, Ω' as its mirror image with respect to the electrode and R as the exterior of $\Omega \cup \Omega'$. Then, by the classical method of images in electrostatics, the capacity can be computed as

$$C = \frac{\varepsilon_0}{2}\int_R |\nabla V|^2\, d\mathbf{x}, \tag{7}$$

where V is an harmonic function outside R decaying at infinity and such that $V = 1$ on the surface of Ω and $V = -1$ on the surface of Ω'. We assume now Ω to be a perturbation of the form (3) of an axisymmetric drop Ω_0. We change variables into a new system $r' = \sqrt{1 + \frac{\varepsilon^2}{2}} r/(1 + \varepsilon \cos(n\theta))$, $\theta' = \theta$, $z' = z$ so that

$$\frac{\partial V}{\partial r} = \frac{\partial V}{\partial r'} \frac{1}{1 + \varepsilon \cos(n\theta')}, \tag{8}$$

$$\frac{\partial V}{\partial \theta} = \frac{\partial V}{\partial \theta'} + \frac{\partial V}{\partial r'} r' \frac{\varepsilon n \sin(n\theta')}{1 + \varepsilon \cos(n\theta')}, \tag{9}$$

and hence, calling R_0 the exterior of $\Omega_0 \cup \Omega_0'$, we have

$$\begin{aligned} C = {} & \frac{\varepsilon_0}{2} \int_{R_0} \left\{ \left| \frac{\partial V}{\partial r'} \right|^2 + \frac{1}{r'^2} \left| \frac{\partial V}{\partial \theta'} \right|^2 + \left| \frac{\partial V}{\partial z'} \right|^2 \right\} d\mathbf{x}' \\ & + \frac{\varepsilon_0}{2} \int_{R_0} \left\{ \frac{2}{r'} \frac{\partial V}{\partial \theta'} \frac{\partial V}{\partial r'} \frac{\varepsilon n \sin(n\theta')}{(1 + \varepsilon \cos(n\theta'))} + \left| \frac{\partial V}{\partial r'} \frac{\varepsilon n \sin(n\theta')}{1 + \varepsilon \cos(n\theta')} \right|^2 \right. \\ & \left. + \left(2\varepsilon \cos(n\theta') + \varepsilon^2 \cos^2(n\theta') - \frac{\varepsilon^2}{2} \right) \left| \frac{\partial V}{\partial z'} \right|^2 \right\} d\mathbf{x}' + O(\varepsilon^3). \end{aligned} \tag{10}$$

We write now $V(r', \theta', z') = V^0(r', \theta', z') + \varepsilon V^1(r', \theta', z')$, where $V^0 = 1$ at the boundary of Ω_0, $V^0 = -1$ at the boundary of Ω_0', $V^1 = 0$ at the boundary of $\Omega_0 \cup \Omega_0'$ and ΔV^0 outside $\Omega_0 \cup \Omega_0'$. Then, from (10) we get

$$\begin{aligned} C = {} & \frac{\varepsilon_0}{2} \int_{R_0} \left| \nabla V^0 \right|^2 d\mathbf{x}' + \varepsilon^2 \frac{\varepsilon_0}{2} \int_{R_0} \left| \nabla V^1 \right|^2 d\mathbf{x}' \\ & + \varepsilon^2 \frac{\varepsilon_0}{2} \int_{R_0} \left\{ \frac{2}{r'} \frac{\partial V^1}{\partial \theta'} \frac{\partial V^0}{\partial r'} n \sin(n\theta') + \left(\frac{\partial V^0}{\partial r'} \right)^2 n^2 \sin^2(n\theta') \right. \\ & \left. + \frac{1}{2} \cos(2n\theta') \left(\frac{\partial V^0}{\partial z'} \right)^2 + 4 \cos(n\theta') \frac{\partial V^1}{\partial z'} \frac{\partial V^0}{\partial z'} \right\} d\mathbf{x}' + O(\varepsilon^3) \\ = {} & C_0 + \varepsilon^2 C_{n,1} + O(\varepsilon^3), \end{aligned} \tag{11}$$

where we used $\int_{R_0} \nabla V^0 \cdot \nabla V^1 d\mathbf{x}' = 0$ and $C_0 = \frac{\varepsilon_0}{2} \int_{R_0} \left| \nabla V^0 \right|^2 d\mathbf{x}'$. From the definition of V^1 and the fact that $\Delta_{\mathbf{x}} V = 0$, it follows

$$\Delta_{\mathbf{x}'} V^1 = -\frac{1}{r'} \frac{\partial V^0}{\partial r'} n^2 \cos(n\theta') - 2 \frac{\partial^2 V^0}{\partial z'^2} \cos(n\theta'), \tag{12}$$

in R_0 with $V^1 = 0$ at the boundary. Since V^0 depends only on (r', z'), we can look for V^1 in the form $V^1 = \cos(n\theta')\Phi(r', z')$ and then

$$C_{n,1} = \frac{\pi\varepsilon_0}{2}\iint\left(\frac{n^2}{2}\left|\frac{\partial V^0}{\partial r'}\right|^2 + \frac{1}{2}\left|\frac{\partial\Phi}{\partial r'}\right|^2 + \frac{1}{2}\left|\frac{\partial\Phi}{\partial z'}\right|^2 + \frac{n^2}{2r'^2}\Phi^2 - \frac{n^2}{r'}\Phi\frac{\partial V^0}{\partial r'} + 2\frac{\partial\Phi}{\partial z'}\frac{\partial V^0}{\partial z'}\right) r'dr'dz'. \tag{13}$$

The integral runs for all values of z'. By Dirichlet's principle, the integral (13) can be characterized as the minimum overall possible Φ of the same integral. Then

$$C_{n,1} = \frac{\pi\varepsilon_0}{2}\min_{\Phi}\iint\left(\frac{n^2}{2}\left|\frac{\partial V^0}{\partial r'} - \frac{\Phi}{r'}\right|^2 + \frac{1}{2}\left|\frac{\partial\Phi}{\partial r'}\right|^2 + \frac{1}{2}\left|\frac{\partial\Phi}{\partial z'}\right|^2 + 2\frac{\partial\Phi}{\partial z'}\frac{\partial V^0}{\partial z'}\right) r'dr'dz'$$

$$\geqslant \frac{\pi\varepsilon_0}{2}\min_{\Phi}\iint\left(\frac{(n-1)^2}{2}\left|\frac{\partial V^0}{\partial r'} - \frac{\Phi}{r'}\right|^2 + \frac{1}{2}\left|\frac{\partial\Phi}{\partial r'}\right|^2 + \frac{1}{2}\left|\frac{\partial\Phi}{\partial z'}\right|^2 + 2\frac{\partial\Phi}{\partial z'}\frac{\partial V^0}{\partial z'}\right) r'dr'dz' = C_{n-1,1}. \tag{14}$$

The later inequality is a simple consequence of the following fact: if a functional F is larger or equal than a functional G when acting on any function Φ, then the minimum of F is larger or equal than the minimum of G. The capacity $C(\varepsilon)$ can be characterized as the minimum of $I = \frac{\varepsilon_0}{2}\int_R |\nabla V|^2 = \varepsilon_0\int_{z>0}|\nabla V|^2$ (by symmetry with respect to the plane $z = 0$) for V such that $V = 0$ at $z = 0$ and $V = 1$ at the surface of Ω. Schwartz's symmetrization principle (see Pólya and Szegö (**8**), the principle stated in VII-3 applies directly to our case) establishes that the minimum of I when the integral is defined over R is larger than the capacity of the symmetrized set that results from replacing each cross-section of Ω and Ω' (orthogonal to the z-axis) with circles of the same area. This process leads to Ω_0 and Ω_0' with capacity C_0. We are going to show that $C_{2,1} > 0$ and, therefore by (14), $C_{n,1} > 0$. Notice that integration by parts, together with the fact that $\Phi = 0$ at $\partial\left(\Omega_0 \cup \Omega_0'\right)$ and $\Delta_{\mathbf{x}'}V^0 = 0$ yield

$$\iint 2\frac{\partial\Phi}{\partial z'}\frac{\partial V^0}{\partial z'}r'dr'dz' = \iint 2\frac{\partial\Phi}{\partial r'}\frac{\partial V^0}{\partial r'}r'dr'dz',$$

and the resulting integrand in (13) can be estimated, for $n = 2$, by

$$2\left|\frac{\partial V^0}{\partial r'}\right|^2 + \frac{1}{2}\left|\frac{\partial\Phi}{\partial r'}\right|^2 + \frac{1}{2}\left|\frac{\partial\Phi}{\partial z'}\right|^2 + \frac{2}{r'^2}\Phi^2 - \frac{4}{r'}\Phi\frac{\partial V^0}{\partial r'} + 2\frac{\partial\Phi}{\partial r'}\frac{\partial V^0}{\partial r'}$$

$$= \frac{1}{2}\left|\frac{\partial\Phi}{\partial z'}\right|^2 + \frac{2}{r'}\Phi\frac{\partial\Phi}{\partial r'} + 2\left|\frac{\partial V^0}{\partial r'}\right|^2 + \frac{1}{2}\left|\frac{\partial\Phi}{\partial r'} - \frac{2}{r'}\Phi\right|^2 + 2\left(\frac{\partial\Phi}{\partial r'} - \frac{2}{r'}\Phi\right)\frac{\partial V^0}{\partial r'} \geqslant \frac{1}{2}\left|\frac{\partial\Phi}{\partial z'}\right|^2 + \frac{2}{r'}\Phi\frac{\partial\Phi}{\partial r'}.$$

Since $\iint \frac{2}{r'}\Phi\frac{\partial\Phi}{\partial r'}r'dr'dz' = 0$, we conclude

$$C_{2,1} \geqslant \frac{\pi\varepsilon_0}{2}\iint \frac{1}{2}\left|\frac{\partial\Phi}{\partial z'}\right|^2 r'dr'dz' \geqslant 0.$$

$C_{2,1}$ could only be 0 if $\Phi = 0$, but then by (13) $C_{n,1}$ would be $\geqslant \frac{\pi\varepsilon_0}{2}\iint 2\left|\frac{\partial V^0}{\partial r'}\right|^2 r'dr'dz' > 0$, which is a contradiction. Hence, $C_{2,1} > 0$. Therefore, the quantities $C_{n,1}$ are strictly positive and increase with n, what proves inequality (6). A more involved proof of (6) was provided in Fontelos and Kindelán (7). An explicit evaluation of $C_{n,1}$ is, in general, only possible by numerical methods. Nevertheless, in the case of flat bodies that are a perturbation of a disk of radius a and with the electrode placed far away ($d \to \infty$, the case considered in Fontelos and Kindelán (7)), a simple scaling argument shows that $C_{n,1}$ are proportional to a. Hence, $C_{n,1}$ increases with a. We believe, from our numerical calculations, this is a general property independently of the distance d at which the electrode is placed, but a mathematical proof cannot be provided at the moment.

The variation of the total energy under the symmetry-breaking perturbation (3) is, by (4) and (5), given by

$$\begin{aligned}\delta E &= \delta A_{lv} - \cos\theta_Y \delta A_{sl} - \frac{1}{2\gamma_{lv}}\delta C V_0^2 \\ &= \varepsilon^2\left[(c_1 n^2 + c_2) - \frac{1}{2\gamma_{lv}}C_{n,1}V_0^2\right] + O(\varepsilon^3). \end{aligned} \tag{15}$$

The constant c_1 will be small if H is small, that is, if the drop is sufficiently flat. For flat disks of radius a, $C_{n,1}$ increases with a (at least if $d \gg 1$). Therefore, for ε sufficiently small, if the drop is sufficiently flat so that $H \ll 1$, then δE may be minimum and negative for some $n > 2$. Hence, a drop perturbed with a $\cos(n\theta)$ mode is energetically more favorable than both the axisymmetric drop and its perturbation with the $\cos(2\theta)$ mode. The formation of multiple fingers is then natural from the energetic point of view. Let us remark at this point that our estimation of relative capacities in (10)–(14) does not rely in the fact that no dielectric is placed between substrate and electrode. If a dielectric layer is introduced, then the capacity is defined by $C = \frac{\varepsilon_0}{2}\int_R \varepsilon_r(z)\,|\nabla V|^2\,d\mathbf{x}$ with $\varepsilon_r(z)$ constant and larger than 1 in the dielectric. Since the region occupied by the dielectric is invariant under the change of variables (3), all the arguments in (10)–(14) are identical, with the only change being a factor $\varepsilon_r(z)$ inside the integrals in (14) and the use of Poisson's equation for V^0 in the form $\nabla_{\mathbf{x}'}\cdot(\varepsilon_r(z')\nabla_{\mathbf{x}'}V^0) = 0$.

To test our calculations and give quantitative estimates, we have computed numerically the equilibrium profiles by solving the Euler–Lagrange equation associated to (2):

$$\gamma_{lv}\kappa - \frac{\sigma^2}{2\varepsilon_0} = -p, \tag{16}$$

where p is the difference of pressure across the interface (which is a Lagrange multiplier associated to the constancy of volume in the minimization problem) and $\sigma = \varepsilon_0\left(\frac{\partial V}{\partial n}\right)$ is the surface charge density. Equation (16) may be further simplified by introducing the changes

$$\mathbf{x} \to (\text{Vol.})^{\frac{1}{3}}\mathbf{x},\ V \to (\text{Vol.})^{\frac{1}{6}}(\gamma_{lv}\varepsilon_0^{-1})^{\frac{1}{2}}V,\ \sigma \to (\text{Vol.})^{-\frac{1}{6}}(\gamma_{lv}\varepsilon_0)^{\frac{1}{2}}\sigma,\ p \to \gamma_{lv}(\text{Vol.})^{-\frac{1}{3}}p, \tag{17}$$

leading to:

$$\kappa - \frac{\sigma^2}{2} = -p. \tag{18}$$

Equation (18) can be considered as an integrodifferential second-order equation: if we denote $h(z)$ as the distance of each point of the drop to the solid substrate, then κ will involve second-order derivatives of h, and σ will result from computing the normal derivative of V, which is a solution of $\Delta V = 0$ with boundary conditions $V = 0$ on the electrode and $V = V_0$ on the drop's surface. We found it convenient to find the solutions to (18) as the stationary solutions of the evolution problem

$$h_t - \Delta\left(\kappa - \frac{\sigma^2}{2}\right) = 0, \tag{19}$$

with boundary conditions

$$h(a) = \frac{\partial}{\partial n}\left(\kappa - \frac{\sigma^2}{2}\right)\bigg|_{r=a} = 0. \tag{20}$$

The surface charge density is computed by using a boundary elements method (**9**) adapted to an axially symmetric geometry. Since $\Delta V = 0$, this amounts to solving, after using the method of images to account for the fact that $V = 0$ at the electrode, the integral equation

$$V^0 = \frac{1}{4\pi\varepsilon_0}\int_\Omega \frac{\sigma(\mathbf{x}')}{|\mathbf{x}-\mathbf{x}'|}d\mathbf{x}' - \frac{1}{4\pi\varepsilon_0}\int_\Omega \frac{\sigma(\mathbf{x}')}{|\mathbf{x}-\mathbf{x}'-2d\mathbf{e}_z|}d\mathbf{x}', \tag{21}$$

for all $\mathbf{x}$ in Ω. In Fig. 3, we represent for given θ_Y and a (radius of the circular solid–liquid interface) the value of the potential V_0 for which the drop spreads that radius a. To construct this plot, we fixed values of V_0, took as an initial drop's shape a spherical cap of unit volume with solid–liquid interface radius a and solved (19) and (20) till we reached a steady configuration. σ was computed by solving numerically the integral equation (21) imposing axial symmetry (which allows to integrate analytically in θ). Once a steady configuration is found, we compute the electric capacity, $C = QV_0$, where $Q = \int\sigma$ is the drop's charge, and the energy rescaled in the new variables defined above: $E = A_{lv} - (\cos\theta_Y)A_{sl} - \frac{1}{2}CV_0^2$, as a function of θ_Y. The energy is written as $E = E_1 - \cos\theta_Y E_2$, where $E_1 = A_{sl}$ and $E_2 = A_{lv} - \frac{1}{2}CV_0^2$. A minimum of energy would correspond to a certain a if $\frac{\partial E}{\partial a} = 0$ or, equivalently, a certain value of a would correspond to a minimizer of the energy if

$$\theta_Y = \arccos\left(\left(\frac{\partial E_1}{\partial a}\right)\Big/\left(\frac{\partial E_2}{\partial a}\right)\right). \tag{22}$$

Therefore, we only need to compute, for given V_0 and varying a, the stationary profiles and their energies E_1 and E_2. We compute their numerical derivatives with respect to a and find θ_Y using (22). The results of Fig. 3 have been computed numerically with this procedure for $d = 0\cdot 5$. In Fontelos and Kindelán (**7**), an isolated drop was considered, which is formally equivalent to making $d \to \infty$. If one takes a particular solid–liquid configuration, and with it a particular θ_Y, then the value of a as a function of V_0 can be found simply by looking at the intersection between the line $\theta_Y =$ constant and the curve corresponding to the given V_0. Notice that the curves $V_0 =$ constant are such that $a \to \infty$ for finite values of θ_Y, which would imply an infinite spreading, for given θ_Y, if V_0 is sufficiently large; just as predicted by Lippmann's law. If one wishes to represent $\theta(V_0)$ as a function of the applied potential V_0 and for a given θ_Y, a horizontal line in Fig. 3 must be traced and its intersections with the curves of constant potential would yield the values of a from which the values of $\theta(V_0)$ would follow under the assumption of a spherical cap drop's geometry. In fact, such assumption is in general incorrect except for sufficiently large values of a. In Fig. 5, we represent

several drop's profiles for a given V_0 together with the theoretical Lippmann's profile, a spherical cap. We remark that the real contact angle is not the apparent $\theta(V_0)$ but θ_Y, with a sharp transition between both angles in a small region near the contact line (**10**).

In Fig. 3, we represent in dashed line, the line to determine the dependence of the drop's base radius a as a function of the applied potential V_0 for $\theta_Y = 1$ radian. The corresponding values of $\cos\theta(V_0)$ (determined from the values of a assuming a spherical cap geometry) are represented in Fig. 4 together with the best fit to a quadratic polynomial and the curve that would correspond to the application of Lippmann's law for the given parameters. As we can see, the results fit very well into a parabolic profile, but which is not exactly the parabola given by Lippmann's law. The reason for this discrepancy lies in the fact that the capacity of the drop electrode system is not exactly the one of a planar capacitor since distance d is comparable to the drop's radius, edge effects become important in the determination of the capacity making it slightly larger (see (**11**)). The increase of the drop's base radius with V_0 is limited by the first bifurcation curve that the dashed line in 3 intersects as a increases. Saturation takes place at this point according to the computations above. At the end of the paper, we will provide also support to our theory through published experimental results (cf. (**12**)).

We implemented a fully three-dimensional boundary elements method to compute energies for nonaxially symmetric drops (details can be found in Fontelos and Kindelán (**7**)). Drops are perturbed sinusoidally in the radial direction, their surface is triangularized (Fig. 2) and their surface charge density is computed by solving the integral equation (21). The thick lines in Fig. 3 delimitate the region where a drop perturbed radially with and n-mode sinusoid is energetically more favorable that the unperturbed drops. Hence, they delimitate the values of V_0 for which circular drops reach saturation so that they cannot spread circularly any further and symmetry-breaking instabilities

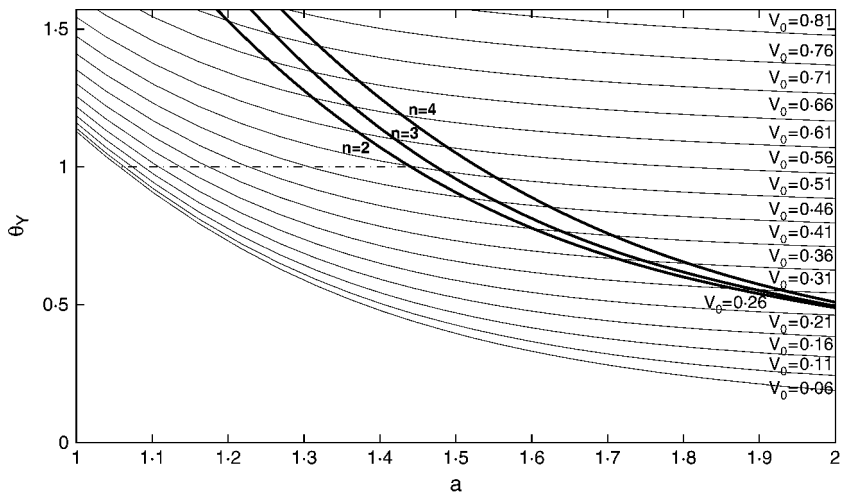

Fig. 3 The bifurcation diagram for $d = 0 \cdot 5$ and a drop of unit volume. The thin curves provide, for given θ_Y and V_0, the radius a to which an axisymmetric drop spreads. The thick lines $n = 2, 3, 4$ delimitate the regions where the drop's shape with n-mode perturbation is energetically favorable with respect to the axisymmetric drop

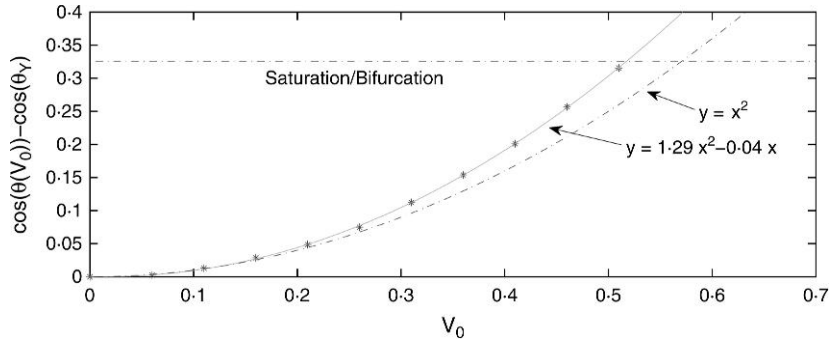

Fig. 4 Representation of $\cos\theta(V_0) - \cos\theta_Y$ as a function of the applied potential V_0 for a drop of unit volume and $d = 0 \cdot 5$. We fit to a quadratic polynomial and compare with the parabola given by Lippmann's law (assuming that the profiles are spherical caps, which is not totally correct unless $d \ll 1$). Saturation occurs when the curve reaches the first bifurcation curve in Fig. 3

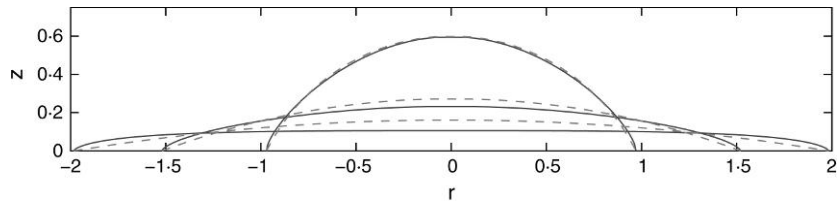

Fig. 5 Drop's profiles (continuous lines) for $V_0 = 0 \cdot 76$ together with spherical cap approximations (dashed lines). The electrode is placed at $d = 0 \cdot 5$. The spherical cap approximation deteriorates as a increases. The drops tend to adopt the form of flat pancakes and close to the contact line a sharp transition between the contact angle θ_Y and $\theta(V_0)$ takes place

emerge. A further increase of the potential may excite higher modes and multiple fingers can emerge from the contact line, as observed in experiments. In fact, we argued above that for sufficiently flat drops, higher order modes lead to more favorable shapes and the appearance of multiple fingers is a reflection of this fact. This is also seen from the fact that the bifurcation curves in Fig. 3 tend to intersect for large values of a. These results have been deduced under a particular kind of perturbation, namely (3). If one considers more general perturbations, instabilities may develop even for smaller values of V_0.

3. Analysis in the neighborhood of the contact line

The perturbation introduced in (3) represents a deformation for any value of z. One would expect that deformations near the solid–liquid interface should have a dominant impact in the overall energy balance since electric field is very intense there. We are going to argue now at the level of a neighborhood of the contact line and for perturbations with a wavelength much smaller than the radius of curvature of the contact line. Hence, we approximate the liquid–vapor interface at a given

point of the contact line by its tangent plane. By introducing local Cartesian coordinates centered at that point, such a plane can be represented as

$$x = (\cot\theta_Y)\, z,$$

and the perturbed interface by

$$x = (\cot\theta_Y)\, z - \varepsilon g(z)\sin(ky), \tag{23}$$

with $g(z)$ such that $g(0) = 1$ and $g(\infty) = 0$. Notice that (23) represents an undulation in the y direction that decays fast as $z \to \infty$. Then, the area created by the perturbation of the planar interface in one y-period $2\pi/k$ will be

$$\begin{aligned}\delta A_{lv} &= \int \left(\sqrt{1 + (\cot\theta_Y - \varepsilon g'(z)\sin(ky))^2 + (\varepsilon k g(z)\cos(ky))^2} - (1 + \cot^2\theta_Y) \right) dydz \\ &\simeq \frac{\pi}{2}\varepsilon^2 k^2 I \sin\theta_Y \equiv c_1 \frac{\sin\theta_Y}{2}\varepsilon^2 k^2, \text{ for } k \gg 1, \end{aligned} \tag{24}$$

where $I = \int g^2(z)dz$. The relative variation of the area of the liquid–solid interface is 0. The contribution to the capacity in a region S, exterior to the volume D delimited by the liquid–solid and the liquid–vapor interfaces and consisting of one y-period and for the points in D such that (x, z) are in a ball of radius R will be given by $\frac{\varepsilon_0}{2}\int_S |\nabla_x V|^2$. By changing variables

$$x' = x + \varepsilon g(z)\sin(ky),$$

we can write

$$\begin{aligned}\int_S |\nabla_x V|^2 &= \int_S \left(\frac{\partial V}{\partial x'}\right)^2 + \left(\frac{\partial V}{\partial x'}\varepsilon k g(z)\cos(ky) + \frac{\partial V}{\partial y'}\right)^2 + \left(\frac{\partial V}{\partial z'}\varepsilon g'(z)\sin(ky) + \frac{\partial V}{\partial x'}\right)^2 \\ &= \int_S |\nabla_{x'} V|^2 + 2\varepsilon \int_S \frac{\partial V}{\partial x'}\frac{\partial V}{\partial y'} k g(z)\cos(ky) + \frac{\partial V}{\partial z'}\frac{\partial V}{\partial x'} g'(z)\sin(ky) \\ &\quad + \varepsilon^2 \int_S \left(\frac{\partial V}{\partial x'} k g(z)\cos(ky)\right)^2 + \left(\frac{\partial V}{\partial z'} g'(z)\sin(ky)\right)^2.\end{aligned}$$

Writing now $V = V^0 + \varepsilon V_1$, with V^0 the potential in the exterior of the unperturbed wedge of angle θ_Y, we get

$$\begin{aligned}\int_S |\nabla_x V|^2 &= \int_S \left|\nabla_{x'} V^0\right|^2 + 2\varepsilon \int_S \nabla_{x'} V^0 \cdot \nabla_{x'} V^1 \\ &\quad + 2\varepsilon \int_S \frac{\partial V^0}{\partial x'}\frac{\partial V^0}{\partial y'} k g(z)\cos(ky) + \frac{\partial V^0}{\partial z'}\frac{\partial V^0}{\partial x'} g'(z)\sin(ky) \\ &\quad + 2\varepsilon^2 \int_S \left(\frac{\partial V^0}{\partial x'}\frac{\partial V^1}{\partial y'} + \frac{\partial V^1}{\partial x'}\frac{\partial V^0}{\partial y'}\right) k g(z)\cos(ky)\end{aligned}$$

$$+\left(\frac{\partial V^0}{\partial x'}\frac{\partial V^1}{\partial z'}+\frac{\partial V^1}{\partial x'}\frac{\partial V^0}{\partial z'}\right)g'(z)\sin(ky)$$

$$+\varepsilon^2\int_S\left(\frac{\partial V^0}{\partial x'}kg(z)\cos(ky)\right)^2+\left(\frac{\partial V^0}{\partial z'}g'(z)\sin(ky)\right)^2+\varepsilon^2\int_S\left|\nabla_{x'}V^1\right|^2.$$

We can write $V^1=\sin(ky')\Phi(x,z)$. The relative variation of capacity will then be, for $k\gg 1$ and letting $R\to\infty$,

$$\delta C=\frac{\varepsilon_0}{2}\int|\nabla_x V|^2-\frac{\varepsilon_0}{2}\int|\nabla_{x'}V|^2$$

$$\simeq\frac{\varepsilon_0}{2}\varepsilon^2\pi\left[k^2\int_W\left(\frac{\partial V^0}{\partial x'}g(z)+\Phi\right)^2+\int_W|\nabla\Phi|^2\right]\equiv\frac{\varepsilon_0}{2}\varepsilon^2\pi\left(\min_\Phi J_k(\Phi)\right),$$

where W is the exterior to the two-dimensional wedge formed by the unperturbed liquid–vapor and liquid–solid interfaces and we have used that all the $O(\varepsilon)$ terms vanish in the limit $R\to\infty$. The reason for this cancellation is that $\int\nabla_{x'}V^0\cdot\nabla_{x'}V^1=0$ and V^0 is independent of y'. Reasoning as in the case of a perturbed axisymmetric drop, it is clear that $\min_\Phi J_k(\Phi)$ increases with increasing k and is positive. We are also able, in this case, to estimate it for large values of k. The equations satisfied by Φ are

$$-\Delta\Phi+k^2\Phi=-k^2\frac{\partial V^0}{\partial x'}g(z)\text{ in }W,$$

$$\Phi=0\text{ in }\partial\Omega.$$

For $k\gg 1$, the solution is $\Phi=-\frac{\partial V^0}{\partial x'}g(z)+O(k^{-2})$ except for a $O(k^{-1})$ thick boundary layer around $\partial\Omega$ where Φ changes, along the curve $\mathbf{x}_0+s\mathbf{n}$ (with $\mathbf{x}_0\in\partial W$ and $\mathbf{n}$ the normal direction to ∂W), from 0 to $-\left.\frac{\partial V^0}{\partial x'}g(z)\right|_{\mathbf{x}_0}$. Along this boundary layer Φ satisfies

$$-\Phi_{ss}+k^2\Phi=-k^2\left.\frac{\partial V^0}{\partial x'}g(z)\right|_{\mathbf{x}_0},$$

$$\Phi(s=0)=0.$$

Then,

$$\Phi(s)=-\left.\frac{\partial V^0}{\partial x'}g(z)\right|_{\mathbf{x}_0}(1-e^{-ks}),$$

and we can approximate

$$\min_\Phi J_k(\Phi)\simeq 2k^2\int_{\partial W}\left(\frac{\partial V^0}{\partial x'}g(z)\right)^2\int_0^\infty e^{-2ks}ds=2k\int_{\partial W}\left(\frac{\partial V^0}{\partial x'}g(z)\right)^2.$$

Hence,

$$\delta C\simeq\varepsilon_0\pi\varepsilon^2k\int_{\partial W}\left(\frac{\partial V^0}{\partial x'}g(z)\right)^2\equiv c_2\varepsilon^2k. \tag{25}$$

Notice that c_1 in (24) may be smaller than c_2 in (25) provided θ_Y is sufficiently small or $\left|\frac{\partial V^0}{\partial x'}\right|$ is sufficiently large. Since $\frac{\partial V^0}{\partial x'} = -E_{x'}$, we conclude that instabilities with large wavenumber are enhanced if electric field is made sufficiently intense close to the contact line.

We conclude then with the following expression for the dispersion relation for periodic perturbations with small wavelength of the contact line:

$$\delta E = \varepsilon^2(\gamma_{lv} c_1 \sin\theta_Y k^2 - \frac{1}{2} c_2 k V_0^2).$$

This formula allows to compute the wavenumber at which the energy decreases most:

$$k_{\max} = \frac{1}{4\gamma_{lv}} \frac{c_2}{c_1} \frac{V_0^2}{\sin\theta_Y}.$$

We can simplify further, using $V^0 = 1$ at ∂W:

$$\frac{c_2}{c_1} = \frac{\varepsilon_0 \int_{\partial W} \left(\frac{\partial V^0}{\partial x'} g\right)^2}{\int g^2(z) dz} = \frac{\varepsilon_0 \int_{lv} \left(\frac{\partial V^0}{\partial x'} g\right)^2}{\int_{lv} g^2 \sin\theta_Y} = \frac{\varepsilon_0 \int_{lv} g^2 \left(\frac{\partial V^0}{\partial n'}\right)^2 \sin^2\theta_Y}{\int_{lv} g^2 \sin\theta_Y} = \frac{\sin\theta_Y}{\varepsilon_0 V_0^2} \frac{\int_{lv} g^2 \sigma^2}{\int_{lv} g^2},$$

and conclude with

$$k_{\max} = \frac{1}{4\gamma_{lv}\varepsilon_0} \frac{\int_{lv} g^2 \sigma^2}{\int_{lv} g^2},$$

a formula valid for small enough wavelengths (much smaller than the radius of curvature of the contact line) and depending solely on the local charge densities near the contact line independent of whether they have been created or amplified by any external element such as electrodes or dielectrics under the substrate.

To summarize, we have explained saturation and instability of spreading droplets in electrowetting as a bifurcation phenomenon by which a drop loses its axial symmetry and develops multiple fingers. We remark that for levitating droplets (which would correspond to the limit $d \to \infty$ and $\theta_Y = \pi$) the appearance of instabilities once a drop has been charged above a critical value is a well-known fact (**13**). In this case, spherical drops when reaching the critical charge become energetically unfavorable with respect to ellipsoidal drops, deform with a $n = 2$ mode and eventually form cone-like singularities at the interface (**14**) with the formation of multiple daughter droplets. Our result serves to connect this behavior with the less understood behavior of drops in electrowetting. The dynamic transition from axisymmetric to multiple finger drop profiles is currently underway (**15**).

4. Connection to experiments

There are already plenty experimental results we can compare our results with. The article (**6**) contains a compilation of results from various other articles and comparison with its authors' own theory. Some of the experimental data available only provide information on the parameters entering in Lippmann's formula (which is incorrect in some regimes) but are missing other parameters such as the volume of fluid deposited on the substrate. In this sense, the data in Blake *et al.* (**12**) are complete and we will use them for our analysis. A 40-μl drop of glycerol solution is deposited onto the surface of a polyethylene terephthalate (PET) film with thickness of $d = 100$ μm, with electric permittivity $\varepsilon_r = 3 \cdot 2$. The surface tension coefficient γ_{lv} is 64 mN/m. Young's angle was found to

be 66°. Given these parameters, one can define a typical length scale l^* as the radius of the drop if it were a sphere, that is, $l^* = 2 \cdot 1 \times 10^{-3}$ m. Hence, the thickness of the PET film is much smaller than the length scale l^* and one can approximate the whole system by a plane capacitor. This fact allows (1) to replace the dielectric of thickness 100 μm with $\varepsilon_r = 3 \cdot 2$ by a dielectric of thickness $100/3 \cdot 2\mu$m with $\varepsilon_r = 1$ and (2) approximate the drops by spherical caps. In Quinn *et al.* (**6**), it was found that the experimental results in Blake *et al.* (**12**) matched almost exactly a law

$$\cos\theta(V_0) - \cos\theta_Y = \beta \frac{\varepsilon_0 \varepsilon_r}{d\gamma_{lv}} V_0^2,$$

with $\beta = 0{\cdot}29$ (remind that $\beta = 0 \cdot 5$ for Lippmann's law) and saturation was reached at about $V_0 = 500$ V with a contact angle of 48°. The value of β obtained is compatible with Lippmann's law if we take

$$\beta \frac{\varepsilon_r}{d} = \frac{1}{2} \frac{1}{d_{\text{eff}}},$$

where d_{eff} is the effective thickness of a dielectric with $\varepsilon_r = 1$ so that the experimental results of Blake *et al.* (**12**) match Lippmann's law. We have computed, for such a dielectric, the energies (2) of configurations with axial symmetry and compared them with the energies of these configurations when symmetry broken in the form explained in previous sections. We write our results in terms of the nondimensional units by changing in the form given by (17) but using as length scale l^* . In particular, the potential we take is $V_0 = l^{*-\frac{1}{2}} (\gamma_{lv} \varepsilon_0^{-1})^{-\frac{1}{2}} V$, where V is the applied potential in physical units, and the energy computed is $E = A_{lv} - (\cos\theta_Y) A_{sl} - \frac{1}{2} C V_0^2$ with C the capacity of the system (in nondimensional units). In Fig. 6, we represent the difference between the energy of the axisymmetric drop and the same drop with the symmetry broken by the $n = 2$ mode, as a function of the potential V_0. The drop with the broken symmetry becomes energetically favorable for $V_0 > 0 \cdot 1658$. In physical units, this is $V > 645$ V. The voltage for which contact angle

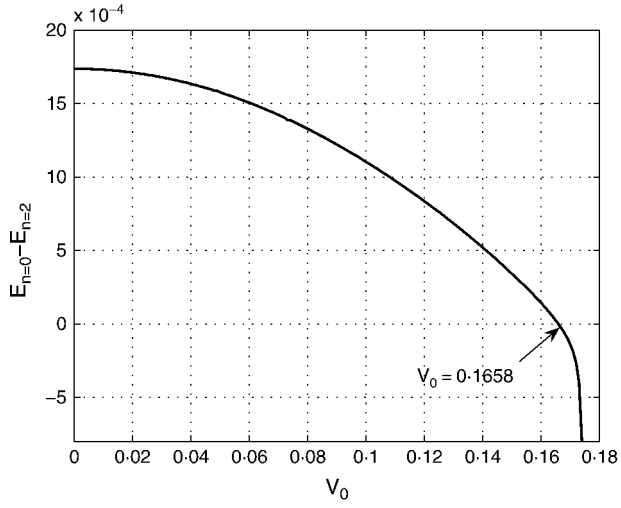

Fig. 6 Difference in energy between the unperturbed axisymmetric drop and the drop perturbed with the $n = 2$ mode, as a function of the applied potential V_0. Notice that bifurcation takes place at $V_0 \simeq 0 \cdot 1658$

saturation was reached in the experiment (**12**) is about 500 V when dc was used, while a slower transition to saturation was observed with ac and, according to Blake *et al.* (**12**), appears to saturate above 600 V.

Acknowledgements

The authors thankfully acknowledge the computer resources provided by the Centro de Supercomputación y Visualización de Madrid (CeSViMa) and the Spanish Supercomputing Network.

References

1. H. A. Stone, A. D. Stroock and A. Ajdari, Engineering flows in small devices: microfluidics toward a lab-on-a-chip, *Annu. Rev. Fluid Mech.* **36** (2004) 381–411.
2. F. Mugele and J. C. Baret, Electrowetting: from basics to applications, *J. Phys. Condens. Matter* **17** (2005) R705–R774.
3. C. Quillet and B. Berge, Electrowetting: a recent. outbreak, *Curr. Opin. Colloid Interface Sci.* **6** (2001) 34–39.
4. L. Yeo and H.-C. Chang, Static and spontaneous electrowetting, *Mod. Phys. Lett. B* **19** (2005) 549.
5. G. Lippmann, Relations entre les phénomènes électriques et capillaires, *Ann. Chim. Phys.* **5** (1875) 494.
6. A. Quinn, R. Sedev and J. Ralston, Contact angle saturation in electrowetting, *J. Phys. Chem. B* **109** (2005) 6268–6275.
7. M. A. Fontelos and U. Kindelán, The shape of charged drops over a solid surface and symmetry-breaking instabilities, *SIAM J. Appl. Math.* **69** (2008) 126–148.
8. G. Pólya and G. Szegö, *Isoperimetric Inequalities in Mathematical Physics* (Princeton University Press, Princeton 1951).
9. C. Pozrikidis, *Boundary Integral Methods for Linearized Viscous Flow* (Cambridge University Press, Cambridge 1992).
10. M. Bienia, M. Vallade, C. Quillet and F. Mugele, Electrical field induced curvature increase on a drop of conducting liquid, *Europhys. Lett.* **74** (2006) 103–109.
11. W. C. Chew and J. A. Kong, Microstrip capacitance for a circular disk through matched asymptotic expansions, *SIAM J. Appl. Math.* **42** (1982) 302–317.
12. T. D. Blake, A. Clarke and E. H. Stattersfield, An investigation of electrostatic assist in dynamic wetting, *Langmuir* **16** (2000) 2928–2935.
13. D. Duft, T. Achtzehn, R. Müller, B. A. Huber and T. Leisner, Coulomb fission: Rayleigh jets from levitated microdroplets, *Nature* **421** (2003) 128.
14. S. Betelú, M. A. Fontelos, U. Kindelán and O. Vantzos, Singularities on charged viscous droplets, *Phys. Fluids* **18** (2006) 051706.
15. C. Eck, M. A. Fontelos, G. Grün, F. Klingbeil and O. Vantzos, A phase-field model for electrowetting, *Interfaces Free Boundaries* **11** (2009) 259–290.